Journal of Physiology (1993), **461**, *pp.* 619–632
With 7 figures
Printed in Great Britain

PERMEABILITY OF DISRUPTED CEREBRAL MICROVESSELS IN THE FROG

BY P. A. FRASER AND ANNABEL D. DALLAS

From the Vascular Biology Research Centre, Physiology Group, Biomedical Sciences Division, King's College London, Campden Hill Road, London W8 7AH

(*Received 13 April 1992*)

SUMMARY

1. This study reports the results of varying the hydrostatic pressure on measurements of permeability coefficient to the low molecular weight impermeant dye carboxyfluorescein (MW = 376) in single leaky cerebral microvessels. A mathematical model, that solved the convective diffusion equations used to analyse the measurements, showed that the measurements were consistent with the leakiness being due to 22 nm wide parallel-sided slits between endothelial cells.

2. Microvessels on the surface of the frog's brain were cannulated with a micropipette and perfused with an artificial cerebrospinal fluid containing the dye. Vessels were occluded with a glass microneedle and the rate of change in dye concentration in a 12 μm length section was measured using video-intensified microscopy.

3. It was found that the rate of dye loss at all points along the occluded microvessel segment could be accounted for by a model for convection and diffusion, and that changes in dye concentration at a point remote from the segment entrance can give a good measure of diffusive permeability.

4. When series of measurements were carried out on a single vessel, permeability rose over the course of 20 min. Mean permeability for all measurements was $3{\cdot}01 \times 10^{-5}$ cm sec^{-1}, $n = 64$ (mode, 2·0; range, 0·48–9·6). The hydrostatic pressure applied during the perfusion had no effect on the measured permeability.

5. The dye concentration along the vessel axis was measured at the steady state and was shown to respond to changes in hydrostatic perfusion pressure in a way predicted by the model. This indicates that hydrostatically driven bulk flow can be important, and thus convection may account for effects previously ascribed to vesicular transcytosis.

6. The possible anatomical basis for the porous pathway is discussed in the light of recent observations on the presence of 0·5 μm perijunctional gaps, the possibility of transendothelial channels, and the unzipping of tight junctions to leave a 22 nm wide slit.

INTRODUCTION

The blood–brain barrier is characterized both by a very low permeability of cerebral microvessels to small polar molecules and ions, and by a hydraulic

conductivity low enough to suggest that the passage of water is largely across cell membranes rather than through a paracellular route (see Fraser, 1992). The barrier can be disrupted in a number of circumstances, for instance by cerebral hypoxia, as a consequence of trauma, hypertension and by the application of hyperosmolar solutions, but the basis of the disruption is not certain. Electron microscopy has shown that endothelial cell vesicle density increases on disruption (see Van Duers, 1980) and this has led to the idea that increased transcytosis is responsible for increased solute transfer from blood to brain. The alternative view is that the leakiness results from the opening up of tight junctions or of a transcellular pathway, which would allow diffusion of solutes coupled to pressure-driven bulk flow.

The physiological evidence is inconclusive. Mayhan & Heisted (1985) found that osmotic barrier opening produced a pattern of escape of different sized macromolecules from the cerebral microcirculation which is consistent with the opening of a diffusive path. In contrast, hypertensive disruption of the barrier did not result in this pattern, and they suggested that this was evidence for vesicular transcytosis. However, it is also possible that the lack of difference in the apparent permeabilities of these molecules is due to solvent drag across relatively wide intercellular gaps. In the experiments described here we have investigated whether changes in hydrostatic pressure result in changes in permeability and solute distribution that are consistent with the presence of water-filled channels large enough to allow significant convection.

A preliminary account of some of these results has been published (Fraser, English & Dallas, 1991).

METHODS

Principles of the Technique

Symbols

A = surface area (cm^2)
$A_p/\Delta x$ = porous area: junction depth per unit area of endothelium (cm^{-1})
c = concentration of carboxyfluorescein (MW = 376) (mmol l^{-1})
C = normalized concentration of carboxyfluorescein
d = diameter of endothelial gap (cm)
D = diffusion coefficient ($cm^2\ s^{-1}$)
J_v = volume flux ($cm^3\ s^{-1}$)
L_p = hydraulic conductivity (cm (cmH_2O s)$^{-1}$)
P' = apparent permeability coefficient (cm s^{-1})
P_0 = diffusive permeability coefficient = $DA_p/\Delta x$ (cm s^{-1})
P_s = convective permeability coefficient = $P_0 Z + J_v(1-\sigma)$ (cm s^{-1})
r = radius of occluded segment (cm)
V = volume of occluded segment (cm^3)
w = junction gap width (cm)
Pe = Peclet number = $J_v(1-\sigma)/P_0$
Z = $Pe/(e^{Pe}-1)$
σ = bulk flow reflection coefficient

We found previously (Fraser & Dallas, 1990) that cannulation and perfusion of frog cerebral microvessels very often resulted in their becoming leaky, presumably representing inflammatory or traumatic disruption of the blood–brain barrier. The same preparation was used to study the effects of changes in perfusion pressure on the rate at which a low molecular weight solute leaked through the disrupted barrier, and as there are many similarities in the analysis of these experiments, the principle features and salient differences only are noted here. A leaky microvessel was cannulated and perfused with physiological solutions containing carboxyfluorescein (MW = 376) and occluded with a glass microneedle. The rate of fall in dye concentration within the trapped

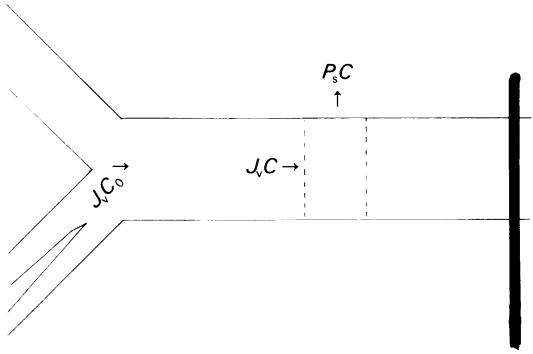

Fig. 1. A schematic diagram of microvessels showing the arrangement of perfusing pipette and occluding microneedle. The pressure in the pipette was adjusted so that blood was displaced from the downstream vessels. This pressure was maintained when one vessel segment was occluded. During an occlusion dye and fluid passed across the whole vessel wall at the rates P_sC and J_v, and were replaced by dye-containing fluid entering from the open end at the rate J_vC_0. The dye concentration was measured from the area outlined by the dotted lines, and here the rate of dye replacement is J_vC.

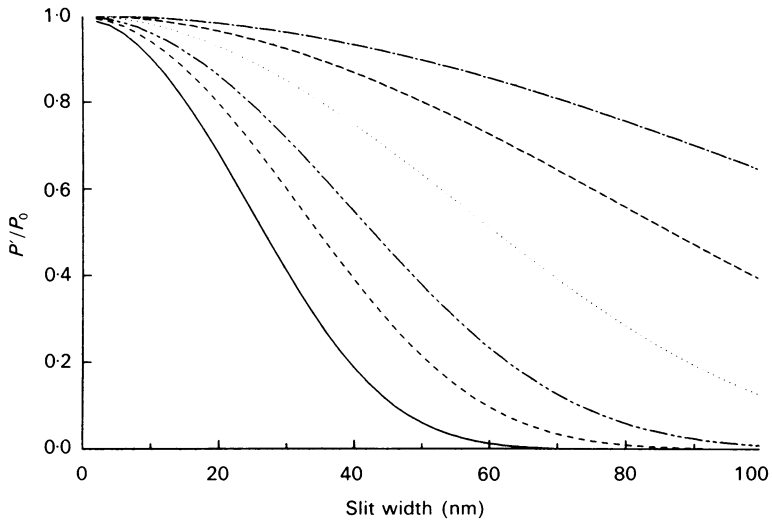

Fig. 2. Plots, based on text eqn (2) and pore theory equations modified for slits (Curry, 1984), showing how the measured permeability P' is thought to decrease as a fraction of the true diffusional permeability as the slit widths and transmural hydrostatic pressures increase. The lines (from top to bottom) give the solutions for pressures of 5, 10, 20, 60, 80 and 100 cmH_2O.

segment was used to measure the permeability coefficient. The cannulation site was close to a bifurcation so that when a downstream microvessel was blocked with an occluding probe the dye concentration at the open end remained constant at the original level (see Fig. 1). The dye concentration was measured in a region close to the occluding probe, but not so close that the vessel diameter was distorted by the occlusion. The boundary conditions for these experiments are that (i) there is no diffusion or flow past the occluding probe, (ii) the dye concentration at the open end of the vessel remains constant, and (iii) the dye concentration immediately outside the vessel wall

is always zero. It was assumed that radial concentration gradients within the occluded segment were small enough to be ignored. There is no continuous cellular layer between these vessels and the superfusing solution (Bundgaard, 1982), so that any dye that crosses the vessel wall is immediately washed away. A transmural hydrostatic pressure gradient will drive fluid across the wall of these leaky vessels and will be replaced by fresh fluid entering the open end of the occluded portion at the original pre-occlusion concentration (C_0). At the steady state, dye concentration in the measured portion will depend on the axial flow as well as the transmural diffusion and flow, but earlier in the occlusion, at points relatively remote from the open ends, the local axial concentration will be uniform. Thus, provided that the permeability is also uniform along the length of the vessel, any fluid lost in a particular region will be replaced by upstream fluid of similar concentration.

Effect of hydrostatic pressure on permeability

A volume flow through a membrane will alter the solute concentration gradient that drives diffusion (Patlak, Goldstein & Hoffman, 1963), and this distortion may be calculated from the Peclet number, the ratio of velocities of solute motion imparted by water motion and by diffusion ($\mathrm{Pe} = J_v(1-\sigma)/P_0$). The term $Z = \mathrm{Pe}/(e^{\mathrm{Pe}}-1)$ shows how the solute concentration gradient at the entrance of a channel falls as water flow increases (Curry, 1984). A convective diffusion coefficient P_s has been used by Huxley, Curry & Adamson (1987) and by Curry, Joyner & Rutledge (1990) in studies of macromolecular efflux from frog mesenteric microvessels, and has been modified for the present experiments, when the dye concentration is measured from within the microvessel, to:

$$P' = P_s - J_v = P_0 Z + J_v(1-\sigma) - J_v, \tag{1}$$

from which:

$$\frac{P'}{P_0} = Z + \mathrm{Pe} - \frac{J_v}{P_0}. \tag{2}$$

P' was determined experimentally from the rate of decrease in dye concentration from the measured segment of the occluded vessel from:

$$C_t = C_0 e^{-kt}, \tag{3}$$

with

$$k = \frac{2}{r} P' t, \tag{4}$$

since the dye concentration immediately outside the microvessel was kept at zero. This apparent permeability P' reduces to diffusional permeability when there is no volume flux. It is possible to produce a plot of theoretical values for P'/P_0 against slit width for different hydrostatic pressures by rewriting eqn (2) in the form $P'/P_0 = Z - \mathrm{Pe}\{\sigma/1-\sigma\}$, and using the modification of the hydrodynamic pore theory derived by Curry (1974, 1984) to estimate σ and Pe. This plot is shown in Fig. 2, from which it can be seen that at a slit width of less than 25 nm, P' for carboxyfluorescein does not fall below 0·6 of the P_0 value, even when the transmural pressure is as high as 100 cmH_2O, and that with more realistic pressures of 20–30 cmH_2O, the value is approximately 0·9.

Effect of hydrostatic pressure on the steady state

At the steady state the dye concentration along the vessel axis will depend on both the rate of dye influx from the open end and the rate of dye efflux across the vessel wall. It was possible to examine this by adapting a mathematical model previously developed and fully described (Fraser & Dallas, 1990) for occlusion experiments on intact cerebral microvessels and those made leaky with hyperosmotic solutions. The model used the value P', measured over a limited section of the occluded segment at the beginning of an occlusion, as a good estimate of P_0 for the whole vessel at all times, and assumed that the diffusive pathway was a slit 22 nm wide. The boundary conditions of the model were that the compartment outside the microvessel was well mixed, its hydrostatic pressure was atmospheric and osmotic pressure was identical to that inside the microvessel. It was also assumed that there was no flow of fluid past the occluding needle, and that fluid entering the occluded section from the open end contained dye at a concentration equal to that inside the microvessel at the start of the occlusion. The only variable which needed to be fitted by trial and error was the transmural hydrostatic pressure gradient.

Experimental protocol

Experiments were carried out using essentially the same techniques as described fully by Fraser & Dallas (1990). Briefly, frogs (*Rana pipiens*) were anaesthetized with 0·2 % ethyl *m*-aminobenzoate (Tricaine) in tap water, the frontoparietal bones were removed and the dura and the arachnoid cut away to leave the surface of the brain exposed. The frog was then placed on the modified stage of a microscope (ACM, Zeiss Oberkochen) and the surface microvessels were viewed through a ×11 Ultrapak objective (Leitz Wetzlar; NA 0·25) fitted with a water-immersion cap to eliminate the air–water meniscus. The surface of the brain was constantly superfused at the rate of 3 ml min^{-1} with an artificial cerebrospinal fluid buffered at pH 7·4 containing (mM): NaCl, 107; KCl, 2; $MgCl_2$, 5; $NaHCO_3$, 5; $CaCl_2$, 2·5; Hepes, 5. The solution used to perfuse the microvessels had a similar ionic composition to the superfusing solution, but also contained the dye 5,6-carboxyfluorescein at 1·06 mM (0·4 g l^{-1}) and bovine serum albumin at 1 g l^{-1}.

Micropipettes (tip diameter, 3–5 μm) and microneedles (tip diameter, 15–20 μm) were held in Leitz micromanipulators to cannulate and occlude selected microvessels. These were venular capillaries of between 12 and 28 μm diameter and were cannulated close to (less than 30 μm) and upstream from a bifurcation. The pressure in the micropipette was adjusted via a manometer so that the flow of carboxyfluorescein was just sufficient to exclude plasma flow from the two vessels. When the manometer pressure was raised the perfusion pressure was expressed as a fraction of the original pressure as no accurate measure of the perfusion pressure at the tip of the pipette could be made. The resistance to flow was assumed to remain constant. The occluding probe was positioned to give a microvascular segment of between 60 and 300 μm length. The microscope image was recorded and analysed in the same way as described by Fraser & Dallas (1990), a cursor on the television monitor determined the area integrated for the video-densitometer, which gave an analog output to a chart recorder. Experiments were recorded on a videotape recorder and analysed later.

RESULTS

The pial microvessels selected for cannulation, perfusion and occlusion were venular capillaries, draining blood from the midline between the lateral cerebral lobes. The dye concentration was measured from a 12 μm length section of the occluded segment, and Fig. 3*A* illustrates the way in which the dye concentration changed with time in such a leaky vessel. The dye concentration fell: initially the rate of decrease was proportional to the concentration, but after the first 20 s it deviated from the simple monoexponential and stabilized, presumably as fresh dye entered the segment from the open perfused end. The fact that dye concentration fell with time indicates that there must be a diffusive pathway, as vesicular transcytosis would be expected to remove dye and solvent at the same rate, thereby leaving no net change in concentration.

Dye concentration was measured at several points along the length of the vessel at various times after the beginning of the occlusion (Fig. 3*B*). The axial distribution follows a pattern that would be expected from convective diffusion across the vessel wall with perfusate containing dye at the original concentration replacing the lost fluid. The computer model (see Methods and Fraser & Dallas, 1990) was used to test this idea by generating curves that should mimic this axial distribution. The model used the value of P' (2×10^{-5} cm s^{-1}) obtained from the monoexponential portion of the curve in Fig. 3*A* and a slit 22 nm wide and 1 μm deep. The steady-state data points were fitted by adjusting hydrostatic pressure in the model by trial and error until a good fit was obtained. The other curves were obtained from exactly the same parameters as the steady-state curve, but with the appropriate times of occlusion. The closeness of the model-derived curves to the data points is encouraging and gives

confidence to the view that a shared convective and diffusive pathway properly describes these leaky microvessels.

Hydrostatic pressure effects on permeability

The effects of altering hydrostatic pressure on the apparent permeability were examined in eleven cerebral microvessels (mean diameter, 14·8 μm; range, 12–17 μm)

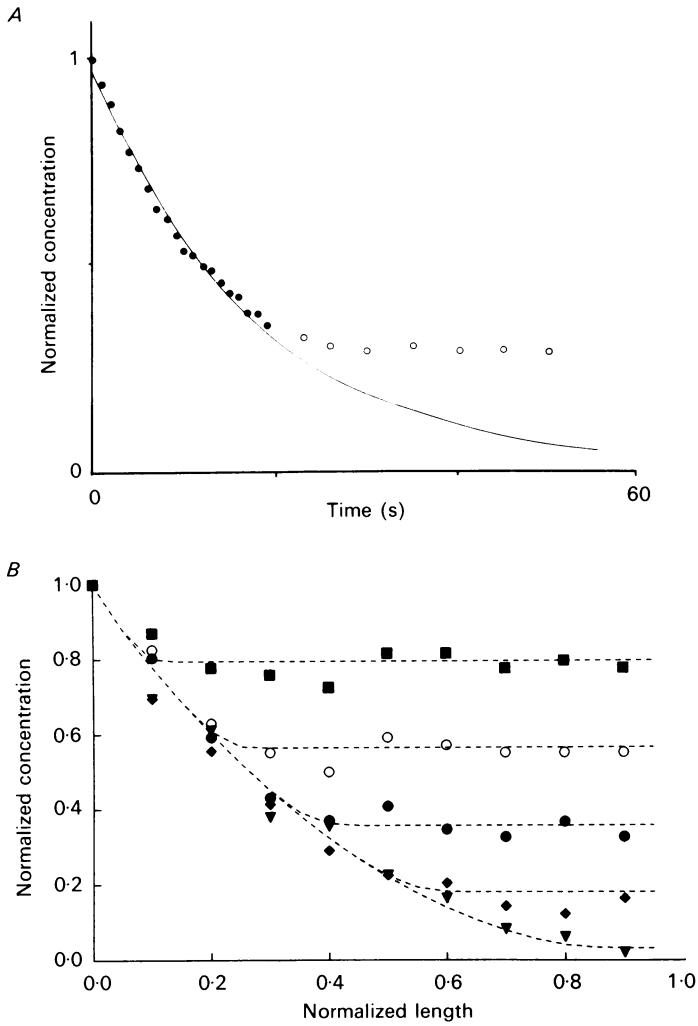

Fig. 3. Changes in dye concentration during an occlusion of a single leaky microvessel. *A*, measured from a 12 μm segment about half-way along a 300 μm length of occluded 14 μm diameter microvessel. The concentration fall followed a monoexponential path for the first 18 s, but then stabilized. *B*, the same occlusion with dye concentration measured at 30 μm intervals along the length of the vessel at 4(■), 10(○), 18(●), 30(◆) and 60(▼) s after the start of the occlusion. The steady state was reached a little before 60 s. The curves were generated from the computer model, the steady state being fitted to a hydrostatic pressure of 45 cmH_2O.

from eleven frogs. The interpretation of these results is complicated by a general increase in permeability as time progressed. Figure 4*A* shows this effect in one vessel and also demonstrates that the changes in measured permeability were not affected by the applied perfusion pressure. Further evidence of the lack of effect of applied

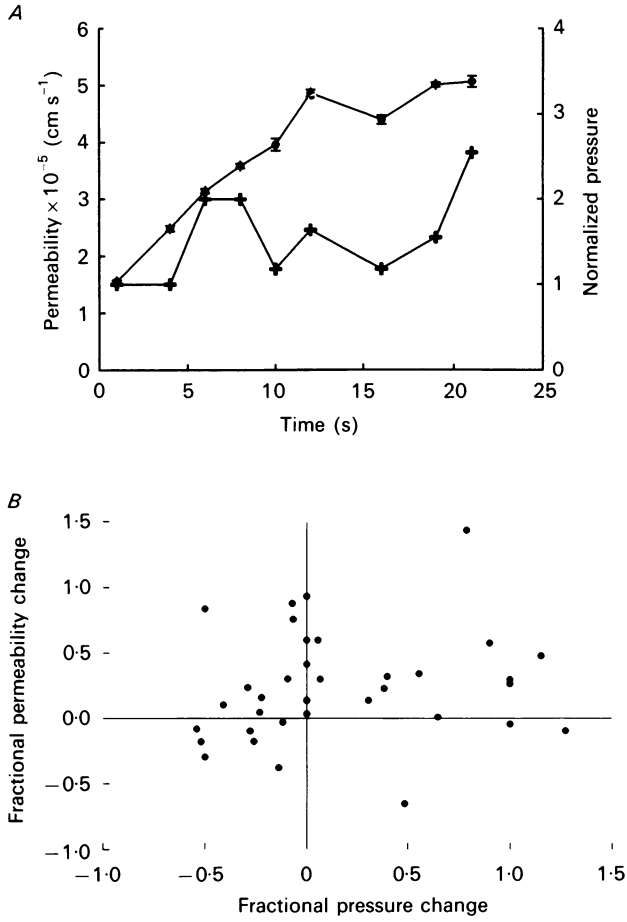

Fig. 4. The effects of perfusion pressure on permeability measurements. *A*, permeability measurements over 22 min carried out on one microvessel. The permeability (●) increased for the first 12 min and then stabilized. The vertical bars indicate the standard error of fitting an exponential to the raw data of a single occlusion. Increases in perfusion pressure, by up to 250 % of the initial value (+), had no apparent effect. *B*, the fractional permeability change from one measurement to the next plotted against the fractional change in hydrostatic pressure in the eleven series of measurements (of which *A* is an example). A negative correlation would be expected if hydrostatic pressure had a significant effect.

perfusion pressure is presented in Fig. 4*B* which summarizes all the vessels studied in which hydrostatic pressure was changed. Each of the eleven vessels was occluded several times with the pressure being changed from one occlusion to another (Fig. 4*A* is an example of such an experiment). If convection were to have a significant effect

on P' a negative correlation between applied hydrostatic pressure and P' would be expected (see Fig. 2). Figure 4*B* shows that there is little correlation between the sequential fractional changes in permeability and in pressure (correlation coefficient $= +0{\cdot}130$ with 38 degrees of freedom).

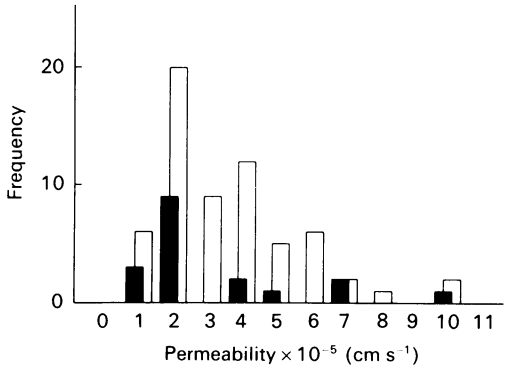

Fig. 5. Frequency distribution of individual permeability measurements. The filled bars show the permeability measurement from first occlusion in any series ($n = 18$), and the open bars show the total of all occlusions ($n = 70$).

As permeability tended to increase with the time of exposure of the preparation it is difficult to give one value that is characteristic of the leaky cerebral venule. The distribution of all the permeabilities measured is shown in Fig. 5; the mode ($2{\cdot}0 \times 10^{-5}$ cm s^{-1}, mean = 3·01, $n = 64$) and range (0·48–9·6 cm s^{-1}) are similar to the mode ($2{\cdot}0 \times 10^{-5}$ cm s^{-1} mean = 4·18, 18 vessels from 13 frogs) and range (0·48–9·4 cm s^{-1}) of the initial values of the same vessels.

Hydrostatic pressure effects on dye distribution

The distribution of dye within the occluded microvessel was examined when the changes in concentration had ceased. At this steady state the dye concentration at any point along the segment will be governed by a combination of its permeation across the wall, and the convective diffusion along the vessel axis. Thus, significant increases in volume flow as brought about by changing the perfusion pressure may be expected to increase the dye concentration at all points along the segment, except of course at the vessel entrance where the concentration is fixed at C_0, and at the point of occlusion where there is no flow and the concentration should be zero (unless there was a leak past the occluding probe). This was borne out in the experiments shown in Fig. 6. Pairs of occlusions in three different vessels were selected such that the measured P' values were similar for both members of the pair while the hydrostatic pressure in the perfusion pipette was significantly different.

The ratios of the hydrostatic pressures were 1:2, 1:1·5 and 1:2 in Fig. 6*A*, *B* and *C* respectively. The dye concentration was raised in each of the occluded segments when pressure was increased. Curves were drawn through the lower sets of points by using the same model as for Fig. 3*B* and the measured P'. A 22 nm slit width was assumed and the pressure parameter was fitted by trial and error (20, 31 and 30 cmH_2O in *A*, *B* and *C*). The upper curves were generated from the same parameters

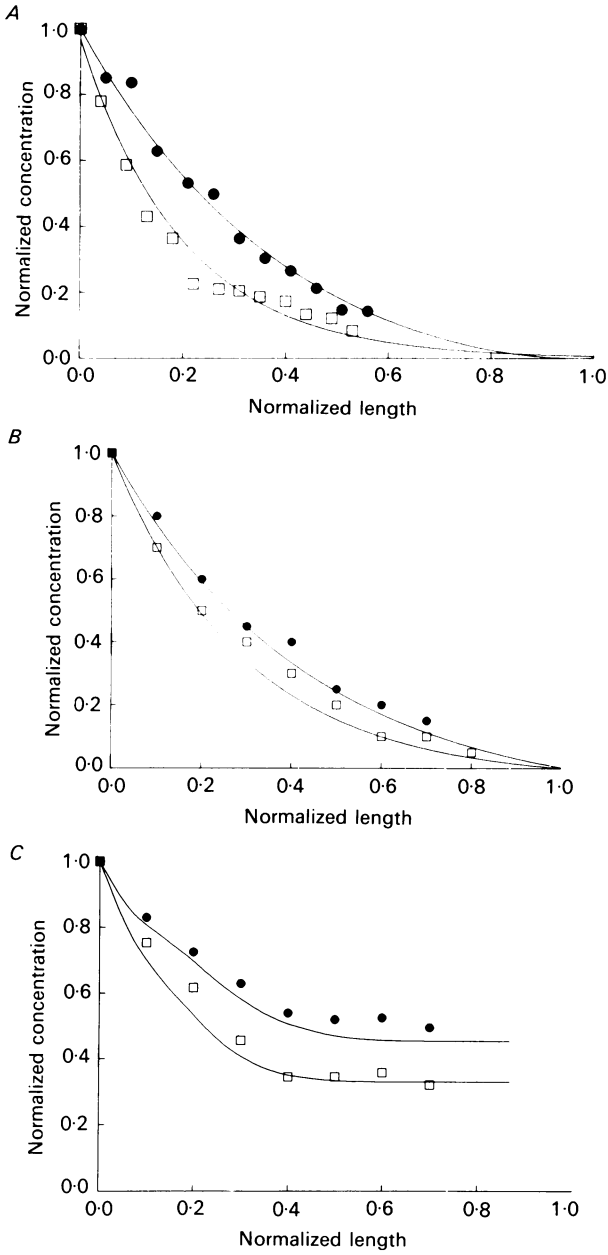

Fig. 6. Axial concentration profiles for three different occluded cerebral microvessels. Each vessel was occluded at two perfusion pressures. The higher pressure (●) was 1:2, 1:1·5 and 1:2 times higher than the lower pressure (□) in *A*, *B* and *C*. The lower lines are best fits using the model with a 22 nm slit and pressures were 20 (*A*), 31 (*B*) and 30 (*C*) cmH_2O. The upper curves were generated from the model and increasing the pressures by the appropriate ratio increases of pressure, viz. 40, 47 and 60 cmH_2O respectively. The whole length of the curves in *A* and *B*, but only the initial part of *C*, were at the steady state.

as the lower curves, except that the pressure parameter was not fitted, but adjusted by the appropriate ratio, so giving an element of verification for the assumptions of the model.

DISCUSSION

The aim of this work was to characterize the permeability in disrupted cerebral microvessels, and it does seem that the results are most simply explained by a pathway shared by water and solutes. Furthermore, this pathway appears to be about 22 nm wide, enough to allow significant convection, but not so wide as to allow the solvent velocity to alter the permeability to small molecules such as carboxyfluorescein. However, there is an alternative which must be considered. These results might be explained by a narrower and longer slit in the vessel wall, which would allow the same diffusive, but little convective solute transfer across the wall, while any water flow would occur mostly as a small leak past the occluding probe. This possibility was tested in the computer model applied to the steady-state experiment illustrated in Fig. 6*A*.

In this simulation (Fig. 7) a 4 nm slit was used, and although the total slit length was adjusted to provide the same diffusive permeability, the filtration coefficient (L_p) was much reduced, owing to the narrowness of the pathway. The total inflow of solution at the vessel entrance was adjusted to that of the 22 nm slit condition by creating a leak past the occluding needle. The low pressure steady-state dye distribution was mimicked by setting the pressure parameter to 6 cmH_2O. When pressure was doubled, the dye concentration close to the occluding probe rose more than that found experimentally. Furthermore, this simulation shows that the higher pressure also resulted in an observable dye flow concentration at the occluding probe, which was never observed in the experiments.

Vesicular transcytosis or convective diffusion?

The presence of significant convection in these disrupted blood–brain barrier venules has implications for the conclusions reached by Mayhan & Heisted (1985). They injected FITC (fluoroscein isothiocyanate)-labelled dextrans (molecular mass, 4, 20 and 70 kDa) into the circulation of rats which had cranial windows that opened on to the cerebral cortex. These windows were superfused and a clearance was calculated from the plasma:superfusate concentration ratios and the superfusate flow. They found that there was no molecular selectivity (clearance ratio 4:70 kDa = 1·2) when rapid acute hypertension (mean arterial pressure, 165 mmHg) was used to disrupt the blood–brain barrier, in contrast to opening the barrier with hyperosmotic shock (clearance ratio, 4:70 kDa = 6·3). They argued that this was evidence for two different types of disruption; vesicular transcytosis being responsible for the disruption in hypertension, and opening of a diffusive path being the basis for the increased permeability with high osmotic pressures. The possibility that hydrostatically driven bulk flow through relatively large spaces would tend to obliterate molecular selectivity was ignored. It is possible to test the bulk flow possibility by calculating P_s (the convective permeability coefficient) from the equations given by Curry and his colleagues (Curry, 1984; Curry *et al.* 1990) in a similar way to Fig. 2. These calculations show that if the permeable pathway were parallel-sided slits 22 nm wide, the ratio of permeabilities measured by Mayhan &

Heisted (1985) would be expected to fall from 5·6 to 3·5, 1·7, 1·4 as hydrostatic pressure rose from 0 to 20, 60, 100 cmH_2O. These calculated ratios are quite close to the experimental ones and give further support to the idea that convective diffusion and not vesicular transcytosis is the correct description for disruption of the

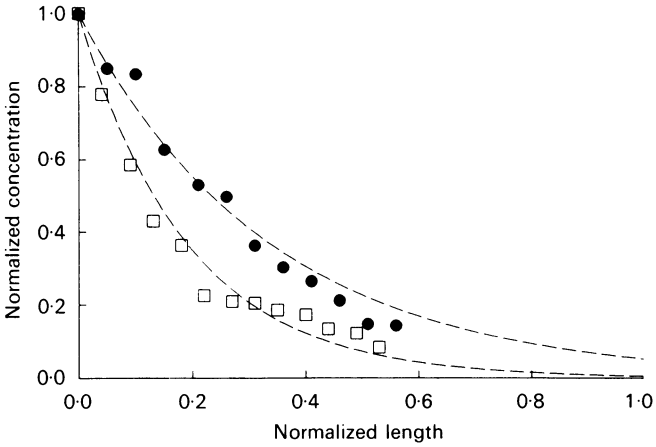

Fig. 7. Axial concentration profile for the same pair of occlusions in Fig. 6*A*. The lower curve was fitted by using the model with a 4 nm slit and a leak past the occluding needle of same magnitude as the total volume flux across the vessel wall for the 22 nm slit condition. The best fit for the lower curve was produced with 6 cmH_2O perfusion pressure. The upper curve was produced with 12 cmH_2O perfusion pressure.

blood–brain barrier. Moreover, Coomber & Stewart (1986) have demonstrated that the appearance of vesicular profiles in electron microscopical sections of blood–brain barrier endothelium is not related to vascular permeability.

Comparison with other permeability measurements in single microvessels

Permeability values from a large variety of sources may be compared by using the parameter $A_p/\Delta x$ (the ratio of junction area to pore depth). This can be derived from the permeability to carboxyfluorescein by assuming a diffusion coefficient similar to that of sucrose (Fraser & Dallas, 1990). In the present study these values (range, *ca* 1–20 cm^{-1}) are comparable to those obtained from frog mesenteric microvessels (Curry, 1979; Curry, Huxley & Adamson, 1983; mean $A_p/\Delta x \approx 28$ and 3·7 respectively).

$A_p/\Delta x$ may also be calculated from the electrical resistance measurements of similar frog pial vessels (Olesen, 1985; Olesen & Crone, 1986; Olesen, 1987*a*, *b*). These were made leaky by anoxia, metabolic inhibitors, oxygen radicals or by the actions of a number of agonists that would be expected to raise intra-endothelial $[Ca^{2+}]$, but these resistance-derived values of $A_p/\Delta x$ were generally much lower than those reported here ($0{\cdot}1 \leqslant A_p/\Delta x \geqslant 0{\cdot}3$). There are a variety of possible sources for this discrepancy, but the two most probable involve the method of measurement and the nature of the permeability change. Firstly, the electrical resistance was estimated from the length constant over several hundred micrometers whereas the present estimates are limited to a 12 μm length of microvessel. Any heterogeneity in the

disruption of barrier properties would tend to decrease the observed resistance value, although in the present experiments there was little evidence for 'hot spots' of raised permeability. Secondly, the resistance decreases occurred rapidly after the application of an agonist and do not necessarily represent significant disruption of the blood–brain barrier. Olesen (1985) noted that there was no apparent leakage of intravascular fluorescein from these vessels, which is consistent with the low permeability that these resistances reflect. This raises the possibility of two forms of disruption of the blood–brain barrier: an initial stage where permeability is intermediate (or $0{\cdot}1 < A_p/\Delta x > 0{\cdot}5$) and a later stage where the permeability is at a level comparable to systemic microvessels ($A_p/\Delta x \geqslant 1$). This view is borne out by results from single pial venules of the rat, where the permeability of tight vessels was observed to increase in two distinct stages (Easton & Fraser, 1992).

Possible porous pathways

The results of these experiments help determine upper and lower limits to the dimensions of the porous path across the endothelium. Figure 2 shows that beyond a theoretical slit width of 30 nm perfusion pressure has significant effects on permeability to carboxyfluorescein, and this gives a theoretical upper limit to slit width. The computer model of the steady-state experiments indicated a lower limit. It was found, as with Fraser & Dallas (1990), that a slit width below 20 nm failed to mimic the dye distribution. This is in accordance with the measurements of Clough & Michel (1988) and of Robinson & Rapoport (1987), and also argues against transendothelial channels formed by a series of fused vesicles (Coomber & Stewart, 1986) as they are equivalent to 70 nm diameter pores.

The various estimates of $A_p/\Delta x$ may also be compared with morphological measurements of Δx and junction length ($\Delta x = 1{\cdot}07\ \mu m$ and $1480\ cm\ cm^{-2}$ respectively; Bundgaard, 1982) combined with the assumed value slit width of 22 nm, thereby giving $A_p/\Delta x_{(morph)} = 30{\cdot}4\ cm^{-1}$, above the maximum value found here. This is consistent with Crone's (1984) suggestion that the porous pathway is formed by the progressive 'unzipping' of the tight junctions, and that the various measures of permeability represent different lengths of open junction.

There is, however, another candidate for the transcellular route. Lossinsky, Pluta, Song, Badmajew, Moretz & Wisniewski (1991) found circular or oval gaps close to the endothelial junctions of about $0{\cdot}5\ \mu m$ diameter in the microvascular endothelium in chronic relapsing experimental allergic encephalomyelitis of the mouse, and suggested that these either form a route for inflammatory cells to cross into brain, or provide anchoring points for these cells as they cause the junctions to open and pass through them. Recently Neal & Clough (1992) showed similar gaps in heat-inflamed frog mesenteric microvessels, but established that this path is associated with a high hydraulic resistance, similar to that found by Clough, Michel & Phillips (1988). Large gaps of about $0{\cdot}5\ \mu m$ diameter filled with a fibre matrix consisting of glycosoaminoglycan (GAG) might satisfy the conditions of the findings of these experiments just as well as a 22 nm slit, so it is important to establish whether cerebral venules have GAG associated with them. Schmidley & Wissig (1986) found that cationized ferritin, a marker for acidic groups at physiological pH, adhered only to non-barrier endothelium in the brain, but it is possible that the process of inflammation results in GAG secretion, as found by Clough *et al.* (1988) who showed

that inflamed mesenteric microvessels secrete Ruthenium Red-staining material. There is also some preliminary evidence from our laboratory to support this view (Easton & Fraser, 1991). Permeability to Lucifer Yellow and rhodamine-labelled albumin, in individual leaky pial venules of the rat, was measured and compared over periods of up to 3 h. The ratio of the permeabilities was often the same as the ratio of the free diffusion coefficients, but at other times the albumin permeability would fall to unmeasurably low values, while the Lucifer permeability remained high. The alternate discharge and removal of GAGs from intercellular clefts may account for these findings.

In conclusion, it has been shown that the leaky microvessels of the disrupted blood–brain barrier have a diffusional path that is shared by water flowing down a hydrostatic pressure gradient, and that this convection can be sufficiently large to explain the lack of molecular selectivity to macromolecules. It is possible that perijunctional gaps have a role to play in the breach of the blood–brain barrier, but the formation of 22 nm slits between previously tight endothelial cell junctions cannot be excluded. Certainly, the range and maximum values for permeability are fully compatible with Crone's 'unzipping' hypothesis, which would leave an open cleft between endothelial cells.

We would like to thank Mr Michael English for help with analysing the data. This work was supported by grants from the Royal Society and the MRC. A. D. D. was an MRC scholar.

REFERENCES

BUNDGAARD, M. (1982). Ultrastructure of frog cerebral and pial microvessels and their impermeability to lanthanum ions. *Brain Research* **241**, 57–65.

CLOUGH, G. & MICHEL, C. C. (1988). Quantitative comparisons of hydraulic conductivity and endothelial intercellular cleft dimensions in single frog capillaries. *Journal of Physiology* **405**, 563–576.

CLOUGH, G., MICHEL, C. C. & PHILLIPS, M. E. (1988). Inflammatory changes in permeability and ultrastructure of single vessels in the frog mesenteric microcirculation. *Journal of Physiology* **395**, 99–114.

COOMBER, B. L. & STEWART, P. A. (1986). Three dimensional reconstruction of vesicles in endothelium of blood–brain barrier versus highly permeable microvessels. *Anatomical Record* **215**, 256–261.

CRONE, C. (1984). Lack of selectivity to small ions in paracellular pathways in cerebral and muscle capillaries of the frog. *Journal of Physiology* **353**, 317–337.

CURRY, F. E. (1974). A hydrodynamic description of the osmotic reflection coefficient with application to pore theory of transcapillary exchange. *Microvascular Research* **8**, 236–252.

CURRY, F. E. (1979). Permeability coefficients of the capillary wall to low molecular weight hydrophilic solutes measured in the single perfused capillaries of the frog mesentery. *Microvascular Research* **17**, 290–308.

CURRY, F. E. (1984). Mechanics and thermodynamics of transcapillary exchange. In *American Handbook of Physiology*, section 2, vol. IV, *Microcirculation*, chap. 8, ed. RENKIN, E. M. & MICHEL, C. C., pp. 309–373. American Physiological Society, Washington.

CURRY, F. E., HUXLEY, V. H. & ADAMSON, R. H. (1983). Permeability of single capillaries to intermediate-sized colored solutes. *American Journal of Physiology* **245**, H495–505.

CURRY, F. E., JOYNER, W. L. & RUTLEDGE, J. C. (1990). Graded modulation of frog microvessel permeability to albumin using ionophore A23187. *American Journal of Physiology* **258**, H587–598.

EASTON, A. S. & FRASER, P. A. (1991). Changes in permeability to large and small molecules in the disrupted blood–brain barrier. *International Journal of Microcirculation: Clinical and Experimental* **10**, 392.

EASTON, A. S. & FRASER, P. A. (1992). Two phases of blood–brain barrier disruption in single cerebral microvessels of the anaesthetized rat. *Journal of Physiology* **446**, 503*P*.

FRASER, P. A. (1992). Diffusional and osmotic permeability to water. In *Handbook of Experimental Pharmacology, Physiology and Pharmacology of the Blood–Brain Barrier*, vol. 103, chap. 3, ed. BRADBURY, M. W. B., pp. 53–64. Springer, Berlin.

FRASER, P. A. & DALLAS, A. D. (1990). Measurement of filtration coefficient in single cerebral microvessels of the frog. *Journal of Physiology* **423**, 343–361.

FRASER, P. A., ENGLISH, M. J. & DALLAS, A. D. (1991). Permeability of single microvessels in the disrupted blood–brain barrier of the frog. *International Journal of Microcirculation: Clinical and Experimental* **10**, 89.

HUXLEY, V. H., CURRY, F. E. & ADAMSON, R. H. (1987). Quantitative fluorescence microscopy on single capillaries: α-lactalbumin transport. *American Journal of Physiology* **252**, H188–197.

LOSSINSKY, A. S., PLUTA, R., SONG, M. J., BADMAJEW, V., MORETZ, R. C. & WISNIEWSKI, H. M. (1991). Mechanisms of inflammatory cell attachment in chronic relapsing experimental allergic encephalomyelitis: a scanning and high-voltage electron microscopic study of the injured mouse blood–brain barrier. *Microvascular Research* **41**, 299–310.

MAYHAN, W. G. & HEISTED, D. D. (1985). Permeability of blood–brain barrier to various sized molecules. *American Journal of Physiology* **248**, H712–718.

NEAL, C. R. & CLOUGH, G. (1992). The changes in hydraulic permeability and porous area of walls of mesenteric microvessels of pithed frogs during acute inflammation. *Journal of Physiology* **452**, 7*P*.

OLESEN, S.-P. (1985). A calcium-dependent reversible permeability increase in microvessels in frog brain, induced by serotonin. *Journal of Physiology* **361**, 103–113.

OLESEN, S.-P. (1987*a*). Regulation of ion permeability in frog brain venules. Significance of calcium, cyclic nucleotides and protein kinase C. *Journal of Physiology* **387**, 59–68.

OLESEN, S.-P. (1987*b*). Free oxygen radicals decrease electrical resistance of microvascular endothelium in brain. *Acta Physiologica Scandinavica* **129**, 181–187.

OLESEN, S.-P. & CRONE, C. (1986). Substances that rapidly augment ionic conductance of endothelium in cerebral microvessels. *Acta Physiologica Scandinavica* **127**, 233–241.

PATLAK, C. S., GOLDSTEIN, D. A. & HOFFMAN, J. F. (1963). The flow of solute and solvent across a two membrane system. *Journal of Theoretical Biology* **5**, 426–442.

ROBINSON, P. J. & RAPOPORT, S. I. (1987). Size selectivity of blood–brain barrier permeability at various times after osmotic opening. *American Journal of Physiology* **253**, R459–466.

SCHMIDLEY, J. W. & WISSIG, S. L. (1986). Anionic sites on the luminal surface of fenestrated and continuous capillaries of the CNS. *Brain Research* **363**, 265–271.

VAN DEURS, B. (1980). Structural aspects of blood–brain barriers, with special reference to the permeability of the cerebral endothelium and choroidal endothelium. *International Reviews in Cytology* **65**, 117–191.